Innovative-SMR Design with CIMBA Fuel using Two-step Code STREAM2D/RAST-K

Wongyu Lee, Wonkyeong Kim, Jinsu Park, Yunki Jo, Jaerim Jang, Eun Jeong, Yeongseok Kang, Kyeongwon Kim, Deokjung Lee*
Department of Nuclear Engineering, Ulsan National Institute of Science and Technology, Ulsan, Republic of Korea
**corresponding author: deokjung@unist.ac.kr*

1. Introduction

To reduce the volume of a reactor core, chemical volume control system (CVCS) that a occupies huge volume in the core should be removed, but this would render soluble boron unusable for controlling excessive reactivity. Without soluble boron, stability, and economic efficiency can be improved because soluble boron causes corrosion in the primary coolant system and negative effect on the moderator temperature coefficient (MTC), and treatment procedure. In this paper, burnable absorber (BA) and control rod operation are used to control excessive reactivity without soluble boron.

A recent report shows innovative BA designs called centrally-shielded burnable absorber (CSBA) which insert various shapes of BAs in UO_2 pellet because spatial self-shielding effect by fuel material slows down the depletion speed of BA in fuel material and makes it possible to control long-term reactivity. CIMBA (Cylindrically Inserted and Mechanically separated Burnable Absorber) is a new type of fuel pin for SMR, cylinder BA composed of gadolinia is inserted in UO_2 fuel to control reactivity, and a detail demonstration is in section 2.1.[1]

Reactor core calculation is performed with two-step code STREAM2D/RAST-K developed at the Ulsan National Institute of Science and Technology (UNIST). STREAM2D is a lattice code that solves transport equations using method of characteristics (MOC) [2]. In STREAM2D, pin-based pointwise energy slowing-down method (PSM) which resolves drawbacks in equivalence theory is used. RAST-K is a nodal code for 3D core calculation. Control rod critical position search with overlap is possible in RAST-K [3].

This paper demonstrates soluble boron free small modular reactor design using STREAM2D/RAST-K. Reactivity is controlled by CIMBA pin and gadolinia pins in design step and excessive reactivity is controlled to critical state by control rod overlapping operation.

2. SMR with CIMBA core design

2.1 Fuel pin design

CIMBA pin is a fuel pin inserted cylindrical BA composed of gadolinia. Natural gadolinia is used, ^{155}Gd and ^{157}Gd ratio is about 30%. Between CIMBA and fuel, a gap filled with air exists. An annular fuel pin is UO_2 fuel pin with 0.075 cm air hole in the center of fuel pin. Gadolinia fuel pin has the same structure in a commercial reactor. ^{235}U enrichment of gadolinia pin is 2.6%, the ratio of gadolinia is different as assembly type.

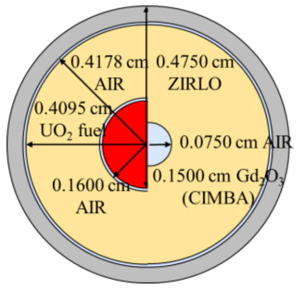

Fig. 1. Structure of CIMBA pin(left) and annular pin(right).

2.2. 2D FA design by STREAM2D

STREAM2D generates a multigroup cross-section for core calculation by solving neutron transport equations using MOC. The fuel assembly (FA) type is 17-by-17 Westinghouse type with 1 instrumental tube and 28 guide tubes. To verify different depletion result as BA, 3 kinds of pin patterns are tested. Fig.2 is pin pattern of each case and Table I is the pin type index. Case 1 is composed of annular pins and gadolinia pins, and case 2 is composed of annular pins and CIMBA pins. In Case 3, CIMBA pins and gadolinia pins are used to control excessive reactivity.

Fig. 2. Pin pattern of fuel assembly (bottom-right 1/4). Case1(left), case 2(center), case 3(right)

Table I: Pin type index

Index	Pin type
1	CIMBA pin
2	Instrumental tube
3	Guide tube
4	Annular pin
5	Gadolinia pin

Fig.3. shows 2D FA depletion result of above cases. Case 1 shows that gadolinia can control excessive reactivity until 23 GWd/MTU. Case 2 shows that

CIMBA can hold down excessive reactivity until 45GWd/MTU, longer than gadolinia pins by spatial self-shielding effect. Case 3 shows that the slope of k_{inf} is changed negative to positive when CIMBA pins and gadolinia pins are used in FA.

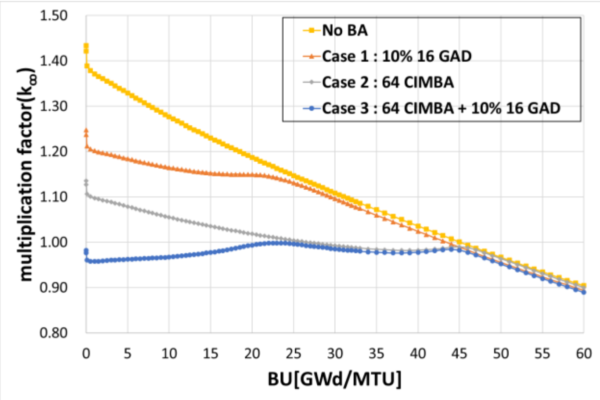

Fig.3. 2D FA depletion result with different BA case.

To verify STREAM2D depletion result, STREAM2D FA depletion result was compared to monte Carlo code, MCS developed in UNIST in Fig.4.[4] 20 million particles were simulated for calculation and the average standard deviation 20 pcm. The root mean square (RMS) for difference is 193 pcm.

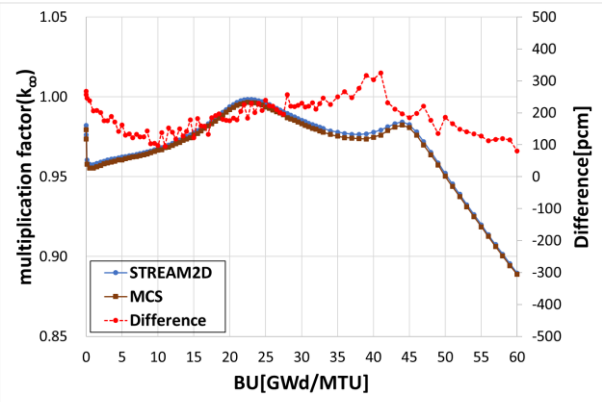

Fig.4. 2D FA depletion comparison STREAM2D and MCS

2.3 SMR with CIMBA core designs

Design parameters for SMR using CIMBA are summarized in Table.1 and table.2 represents target parameters of interest for SMR with CIMBA design. To confirm reactivity hold-down effect by CIMBA and gadolinia pin, multiplication factor (k_{eff}) should be within range in all rod out (ARO) depletion. Because control rods are inserted from top to bottom during control rod overlapping operation, power is concentrated to bottom. To check power tilt caused by control rod, 3D pin peaking factor (F_q) and axial shape index (ASI) was considered during control rod overlapping operation.

For stable excessive reactivity control with control rod, to maintain consistent differential rod worth is important. Without control rod overlap, differential rod worth is decreased after control rod is inserted more than half of active fuel height in reactor which has cosine shape of axial power distribution.[5] In this reason, control rod overlap is tested with half of active fuel height, 120 cm.

Table II: Design parameter for SMR with CIMBA

Parameter	Value
Thermal power [MWth]	540
Fuel enrichment [w/o ^{235}U]	4.95
Fuel pin types	- CIMBA pin - Annular pin - Gadolinia
Number of FA in core [-]	69
Control rod material	AIC
Control rod overlap [cm]	120
Inlet temperature [K]	568.65
Reflector material	Stainless steel
Cladding material	ZIRLO
Active fuel height [cm]	240

Table III: Target parameter for SMR with CIMBA

Target parameter	Range
k_{eff}	$1.005 < k_{eff} < 1.015$
F_q	$F_q < 2.0$
ASI	$-0.3 < ASI < 0.3$

Fig.5 is the loading pattern (LP) for SMR with CIMBA and control rod bank. Control rod banks for control excessive reactivity are R4 and R3 in Fig.5. After inserting the R4 control rod first, R3 control rod is inserted with 120 cm height difference. In the following figures, the vertical lines indicate R4 control rod bank position, and horizontal lines indicate R3 control rod bank position. Fig.6 shows axial composition of each fuel assembly in loading pattern. The number of each BA pins is represented in Fig.6. In Fig.5 and Fig.6, the number of loaded CIMBA was different to prevent concentration of power. In radial direction, the number of CIMBA in the center of reactor core is higher. In axial direction, CIMBA were more in lower part than upper part so that power from lower part can be controlled by CIMBA fuel if power is concentrated to lower part because of control rod insertion.

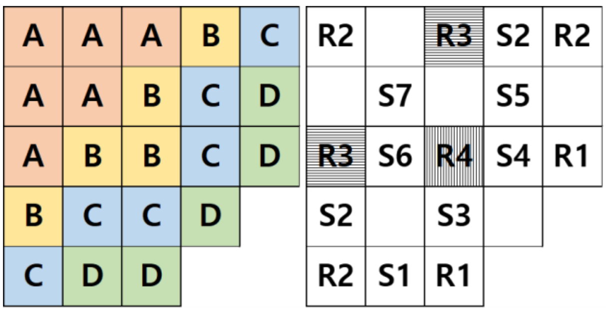

Fig. 5. Loading pattern(LP) and control rod bank

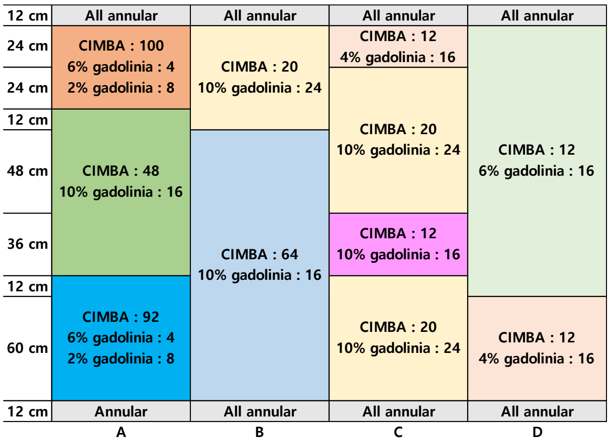

Fig. 6. Axial composition of FA.

3. Result

Reactor core calculation is conducted with thermal/hydraulic (TH) feedback. TH1D calculation is conducted considering gadolinia in CIMBA pin and air hole in annular pin.

Fig.7 shows SMR with CIMBA core calculation result by RAST-K, k_{eff} in ARO case, and control rod critical position for each burnup. Discharging burnup is 20.7 GWd/MTU, about 758 days.

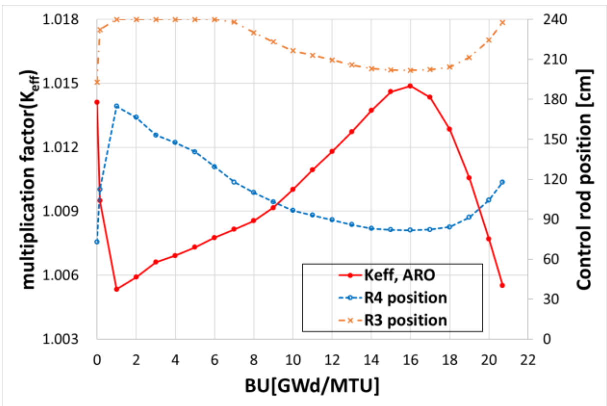

Fig.7. core calculation result, k_{eff} and CR position.

Fig.8 and Fig.9 represent ASI and F_q as depletion. In Fig.8, power from the upper part shows higher than the lower part in ARO case. After control rod insertion, power was tilted to the lower part, ASI changed from negative to positive value, which means the power was tilted to lower part because of control rod insertion. In fig.9, F_q is increased after rod operation, but it is lower than the target parameter. The F_q peak position is located next to the R4 control rod bank critical position. Control rod insertion has a significant impact on the power distribution in the reactor core.

To check the effects of control rod insertion on the power distribution, radial and axial power distribution is compared at the most control rod insertion. At BOC, control rod was most inserted, control rod bank 1 is inserted to 72.83 cm and control rod bank 2 is inserted to 192.83 cm.

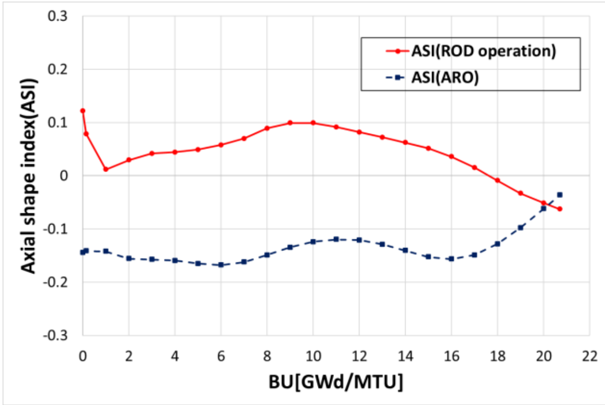

Fig.8. ASI as depletion ARO and ROD operation.

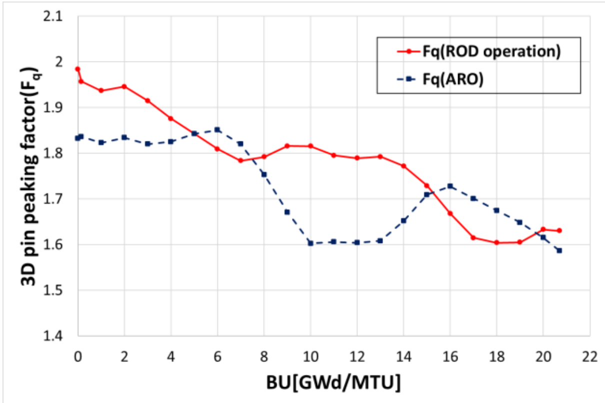

Fig.9. F_q as depletion ARO and ROD operation.

Fig.10 shows radial power distribution at BOC as control rod insertion. As intended in the design step, power from the center of core is lower in ARO case. After control rod insertion, FA power at CR1 bank decreased about 27%, 1.05 to 0.76.

0.84	0.86	0.95	1.04	0.94
0.86	0.89	0.98	1.17	1.03
0.95	0.98	1.05	1.14	0.87
1.04	1.17	1.14	0.94	
0.94	1.03	0.87		

0.84	0.85	0.88	1.08	1.03
0.85	0.86	0.92	1.2	1.12
0.88	0.92	0.76	1.13	0.93
1.08	1.2	1.13	0.96	
1.03	1.12	0.93		

Fig.10. Radial power distribution at BOC ARO(left) and rod operation(right).

Fig.11 shows axial power distribution at BOC with and without control rod insertion and control rod position. Without control rod, power from upper part is higher than lower part but after control rod insertion, with control rod overlapping operation and ARO case. Because of the heterogeneous axial composition of FA, axial power is tilted to top without control rod but after control rod insertion, power from the upper part decreased and power from the lower part is increased. After reactor operation with control rod, Fig.12. shows axial power distribution at EOC with and without control rod. A similar tendency as seen at BOC is also observed during EOC.

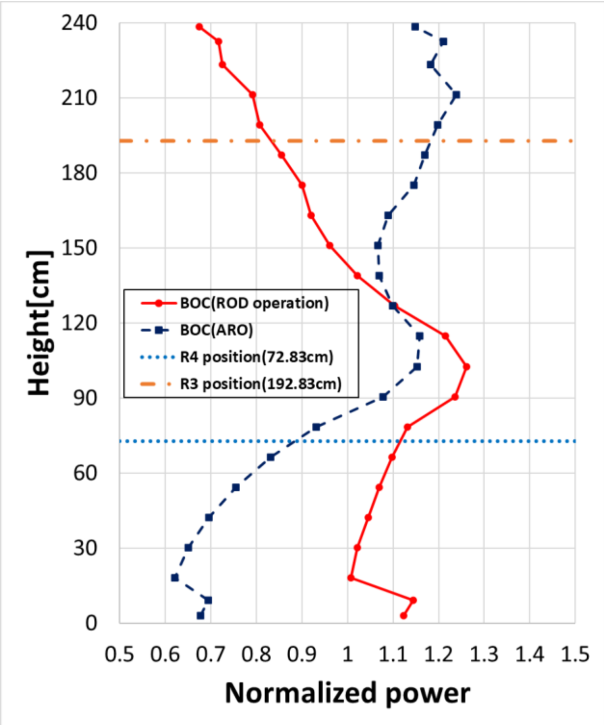

Fig.11. Normalized axial power distribution at BOC and control rod position.

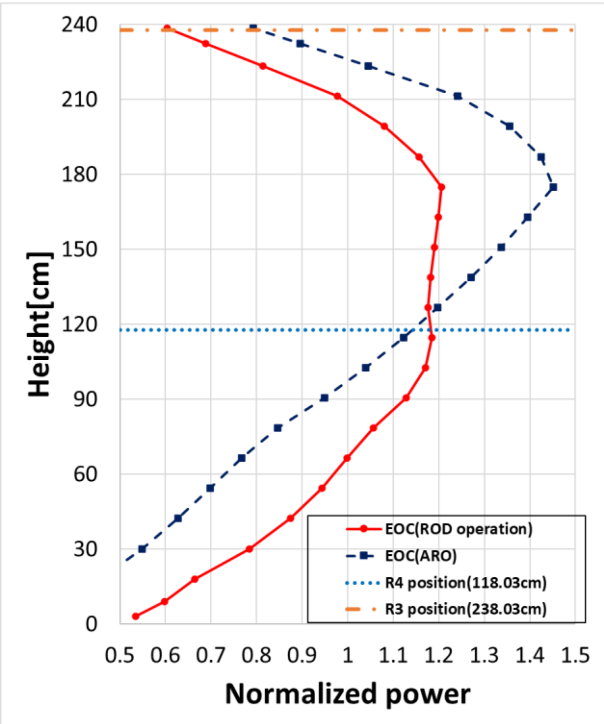

Fig.12. Normalized axial power distribution at EOC and control rod position.

Fig.13 shows radial burnup distribution at EOC after reactor operation with control rod. FA which was inserted control rod shows the lowest burnup 17.1 GWd/MTU, and maximum was near the control rod bank, 24.5 GWd/MTU. The average burnup is 20.7GWd/MTU (758 days).

18.5	18.8	19.9	22.7	20.6
18.8	18.8	20.0	24.5	22.0
19.9	20.0	17.1	22.9	18.4
22.7	24.5	22.9	19.2	
20.6	22.0	18.4		

Fig.13. Radial BU distribution at EOC.

4. Conclusion

In this paper, soluble boron free SMR with CIMBA was designed by two-step code STREAM2D/RAST-K. To control excessive reactivity without soluble boron, gadolinia, CIMBA and control rod were used. To prevent power tilt caused by control rod operation, BA are loaded more in lower part of the reactor core than upper in design step, so that axial composition of FA becomes heterogeneous. In operation step, excessive reactivity was controlled by control rod overlap. The result met the design target parameter, k_{eff}, ASI, and F_q. the discharging BU is 20.7 GWd/MTU and effective full power day (EFPD) is 758 days.

As future works, the design of SMR with CIMBA should be made more realistic by considering multicycle design to increase fuel efficiency, simplification of FA axial design to ensure fuel feasibility, and the effects of control rod depletion caused by control rod insertion operation. To reach the fuel discharging BU as a commercial reactor, the multicycles operation for using fuel efficiently should be considered. To simplify the fuel rod axial composition within a manufacturable range, the FA axial design needs to be simplified. Additionally, the effects of control rod insertion on the flux spectrum and the change in the composition of the control rod due to depletion should be considered for more accurate core depletion calculation.

ACKNOWLEDGEMENT

This study was sponsored by the Korea Hydro & Nuclear Power Co.'s affiliated Central Research Institute (KHNP-CRI).

REFERENCES

[1] YuGwon Jo, and Ho Cheol Shin, Design optimization of cylindrical burnable absorber inserted into annular fuel pellets for soluble-boron-free SMR, Nuclear Engineering and Technology, Vol.54, pp.1464-1470, 2021.

[2] Jiwon Choe, Sooyoung Choi, Peng Zhang, Jinsu Park, Wonkyeong Kim, Ho Cheol Shin, Hwan Soo Lee, Ji-Eun Jung,

and Deokjung Lee, Verification and validation of STREAM/RAST-K for PWR analysis, Nuclear Engineering and Technology, Vol.51, pp.356-368, 2018.

[3] Sooyoung Choi, Changho Lee, and Deokjung Lee, Resonance treatment using pin-based pointwise energy slowing-down method, Journal of Computational Physics, Vol.330, pp.134-155, 2017.

[4] Hyunsuk Lee, Wonkyeong Kim, Peng Zhang, Matthieu Lemaire, Azamat Khassenov, Jiankai Yu, Yunki Jo, Jinsu Park, and Deokjung Lee, MCS – A Monte Carlo particle transport code for large-scale power reactor analysis, Annals of Nuclear Energy, Vol.139, 2018.

[5] Jaeseung Song, Byeongo Jo, and Sungkyun Zee, Optimization of Control Bank Overlap for SMART, KAERI/TR-1148/98,1998.